Industrial Chemistry & Materials

ROYAL SOCIETY OF CHEMISTRY

PAPER

View Article Online
View Journal | View Issue

Cite this: *Ind. Chem. Mater.*, 2024, **2**, 154

Preparation of carbon nanotube-reinforced polyethylene nanocomposites with better anti-scaling and corrosion-resistant properties

Binbin Sun,†[a] Qian Liu,†[b] Yuxin Gao,[a] Liang Han,[b] Rui Zhang,[a] Chenxi Zhang[c] and Xilai Jia *[b]

Anti-scaling technology for pipelines has always been a focus of oilfield industrial production. Compared with traditional metal pipes, polyethylene (PE) pipes have unique advantages in terms of corrosion resistance, surface friction resistance, and service life. In this paper, aiming at an enhancement of anti-scaling and corrosion-resistant properties, as well as increased mechanical properties, PE nanocomposites have been prepared by the introduction of modified carbon nanotubes (m-CNTs) into the PE matrix. To improve the interface compatibility of the composites, the CNTs were treated with reactive tetrabutyl titanate after nitric acid oxidation, which brings about uniform dispersion of the CNTs and intimate interface interaction. As the m-CNT fraction increases, the PE crystallinity displays a slight increase. Polarized microscopy shows that the scaling on the surface of the composite material is obviously reduced compared with pure PE, because the surface free energy of the composite material decreases. Moreover, due to the good dispersion, the composites show enhanced mechanical properties. That is, by adding 1.10 wt% CNTs, the tensile stress and impact toughness of the composites are 20.76 MPa and 37.89 kJ m^{-2}, respectively, increases of 15.0% and 11.9% compared with pure PE. This paper supports the idea that the crystallinity of the PE matrix can be improved by adding CNTs, thereby increasing the corrosion resistance and anti-scaling properties. This work can provide inspiration for using the methods of scale inhibition and corrosion resistance in polymer nanocomposites.

Received 14th March 2023,
Accepted 20th June 2023

DOI: 10.1039/d3im00031a

rsc.li/icm

Keywords: Carbon nanotube; Nanocomposite; Polyethylene; Anti-scaling; Corrosion-resistant.

1 Introduction

Pipeline scaling is a common problem in the petroleum industry.[1–4] Scale in the pipeline can narrow the area of the cross-section of the conduits and increase the resistance to fluid transport.[5,6] Therefore, it is desirable to pay more attention to anti-scaling technology. The formation of scale is mainly due to the precipitation of inorganic salts such as calcium carbonate, calcium sulfate and magnesium hydroxide.[2,7] By preparing or coating materials with low surface free energy on the surface of metal pipelines, the difficulty of adhesion of scale to the surface is increased.[8] Due to their low surface free energy and very convenient processing technology, various kinds of polymeric materials have been widely used in coating the inside of the pipelines and they show unique advantages in self-cleaning and anti-corrosion.[9–11] However, the mechanical strength and hardness of most polymers are poor due to their intrinsic properties, which limits their broader application in pipelines.[12] Therefore, the addition of various fillers to a polymer to improve its mechanical and functional properties and broaden its application range has been a research hotspot.[13–19]

Among the vast number of polymers, polyethene (PE) has been widely used in pipelines in the petroleum industry due to its low cost, facile processability, and moisture resistance. It can be high-crystalline, low-crystalline or amorphous.[20] The modulus and strength of many of these materials are relatively low, which means that, besides electrical conductivity, other properties such as mechanical properties can also be significantly enhanced after adding nanofillers.[21–28] In the harsh fluid environment in oilfield industrial production, PE pipe materials are easily eroded mainly from amorphous cracks to the whole, which leads to

[a] *Daqing Petrochemical Research Center, Daqing, Heilongjiang 163714, China*
[b] *School of Materials Science and Engineering, University of Science and Technology Beijing, Beijing 100083, China. E-mail: jiaxl@ustb.edu.cn*
[c] *Beijing Key Laboratory of Green Chemical Reaction Engineering and Technology, Department of Chemical Engineering, Tsinghua University, Beijing 100084, China*
† These authors contributed equally.

frequent replacement. If a facile and simple method can be used to increase the the crystallinity of the PE matrix, the corrosion resistance of the pipes is expected to be improved.

On the other hand, pipeline scaling has always been a serious problem. The water of oil injection wells is rich in various minerals.[29–31] When the temperature, pressure and pH value change, scale is easily formed and it becomes a challenging task to remove the complex scale. In order to improve the anti-scaling performance and durability of coating materials based on PE polymers, nanocomposite materials have been made by introducing various kinds of nanofiller in an appropriate proportion. At present, researchers are committed to preparing polymer composites with both mechanical properties and scale inhibition performance. By adding various fillers into the polymer matrix, the defects of poor rigidity, hardness, and impact resistance of the polymer matrix have been proved to be improved in many studies.[21,32–34] For instance, due to their reduction ability and barrier performance, graphene and some other two-dimensional nanosheets have been introduced to polymers as an effective anticorrosion coating, which can bring about enhanced mechanical strength and anti-scaling.[35–38] Among nanofillers, CNTs have a specific one-dimensional structure in comparison with other dimensional nanofillers. Moreover, compared to graphene, the dispersion of CNTs has been scaled up, and the reduction in its price makes it possible for CNTs to be added into PE nanocomposites on a large scale.[35,39–41] Due to their outstanding properties, especially high electrical conductivity and mechanical strength, it is found that the addition of such a 1D nanofiller can bring about an obvious enhancement in the mechanical properties and electrical conductivity of the nanocomposites.[42–49] Despite a lot of literature on CNT/PE nanocomposites being reported, there are almost no reports concerned with the effect of carbon nanotubes on the anti-scaling and corrosion resistance of PE nanocomposites.[11,14,15,50–55] Besides, CNTs can be functionalized and dispersed in some polymers for coating applications,[56] like typical CNT-filled epoxy-based nanocomposites.[57] Such a nanocomposite coating can bring about improved anti-corrosion ability in comparison with pure epoxy coating. However, the coating layer may encounter problems of peeling.

In this work, we report PE nanocomposites with excellent anti-scaling performance, which are fabricated by incorporating CNTs. To improve the interface compatibility of the composites, the CNTs were treated by nitric acid oxidation followed by reactive tetrabutyl titanate. Unlike previous modification methods, this paper provides a strategy which can also effectively disperse the CNTs with high aspect ratios in the PE matrix, resulting in intimate interfacial interactions. More importantly, this work reveals that the crystallization of PE can be increased by increasing the fraction of CNTs, leading to higher PE crystallinity and better corrosion resistance. Moreover, due to the good dispersion, the composites show enhanced mechanical properties. This is superior to many CNT–polymer nanocomposites that may show decreased mechanical strength due to the addition of a high content of nanofillers.[58] The work here provides a simple yet effective method for research into scale inhibition and corrosion resistance.

2 Results and discussion

Fig. 1a shows the preparation steps for the m-CNTs. Due to the existence of defects, the surface of the CNTs can be oxidized with nitric acid to produce reactive groups like –OH and –COOH. After that, the surface of the CNTs is reacted with tetrabutyl titanate molecules. Fig. 1b compares optical photographs of the original CNTs and m-CNTs in ethanol, with a weight fraction of 0.2 wt%. After standing for two hours, the primary CNTs become agglomerated and precipitate to the bottom, while the m-CNTs can still retain a uniform dispersion, indicating that the dispersion of CNTs after modification has been obviously improved. This is expected to improve the interfacial bonding of the CNTs with polyethylene due to the grafted alkyl groups. Fig. 1c shows the SEM image of the m-CNTs. After treatment with HNO_3 for 1 hour and reactive tetrabutyl titanate, the aggregated state of the CNTs had been broken, and the CNTs still maintained a large aspect ratio. Fig. 1d and e display the TEM images of the m-CNTs. A small amount of coating layer has been attached to the surface of the CNTs treated with tetrabutyl titanate, which may be the groups of –Ti–O–CH_2–CH_3 and partial TiO_2. The element distribution mapping also showed that Ti and O were evenly encapsulated around carbon.[59] This is consistent with the surface modifications of the CNTs, as illustrated in the experiments.

According to a comparison of the Raman shifts of the CNTs during the modification steps (Fig. 2f), the ratio of the D peak to the G peak (I_D/I_G) of untreated CNTs is about 0.96, while those of the oxidized CNTs and m-CNTs are 0.84 and 0.67, respectively. This indicates that the acidification and grafting treatments cause no great damage to the nanotubes, and this functionalization method shows no great damage to the structural integrity of the nanotubes. Good retention of the structural integrity of the carbon nanotubes is beneficial to maintaining their good mechanical and thermal conductivity.

Fig. 3a shows that the typical diffraction peaks of the CNT filler are located at 25.8° and 43.2°, corresponding to the (002) and (100) crystal planes, respectively. The results support the crystal structure of the carbon nanotubes still remaining after modification. Moreover, close to the (002) peak of the CNTs, a small peak at around 26.2° can be observed which should be ascribed to the (101) peak of TiO_2. This indicates that a small fraction of tetrabutyl titanate might be converted to TiO_2 on the CNTs during the modification. The XRD characterization of PE before and after the introduction of the CNTs are compared in Fig. 3a. PE shows obvious peaks at 21.5° and 23.9°, which are characteristic diffraction peaks of (110) and (200) crystal

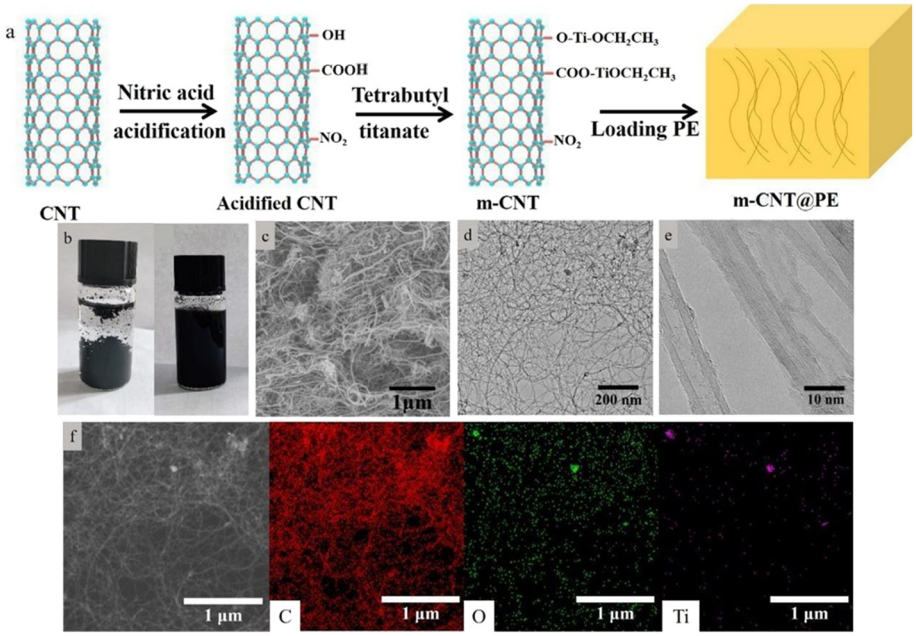

Fig. 1 (a) Schematic diagram of surface modification steps with CNTs to make PE nanocomposites. (b) Comparison of optical photographs of the original CNTs and m-CNTs in ethanol. (c) SEM and (d and e) TEM images of the m-CNTs. (f) Elemental mapping of the m-CNTs.

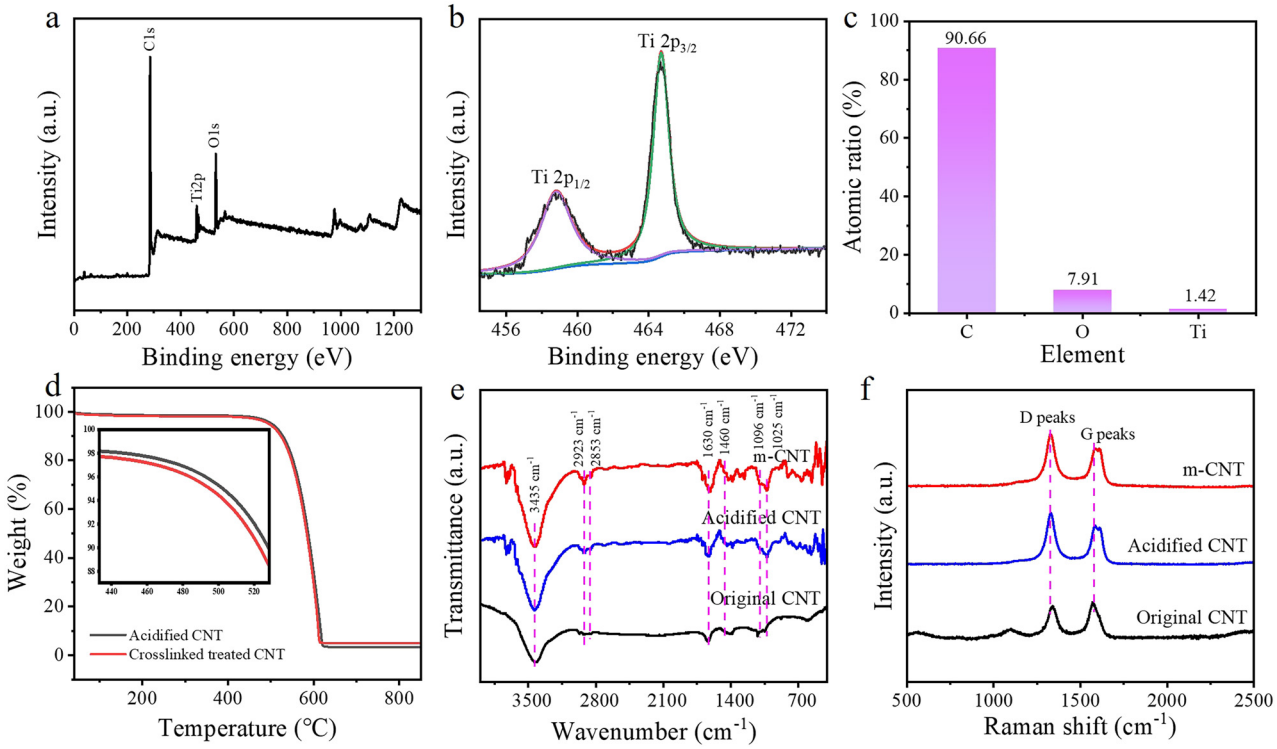

Fig. 2 (a–c) XPS Ti2p spectra of the m-CNTs. (d) TGA curves of the acidified CNTs and m-CNTs. (e) FTIR and (f) Raman shifts of the different CNT samples.

planes, respectively, which proves that it contains a partially crystalline structure. The results show that the characteristic peak of PE is still maintained after adding the m-CNTs, but the peak of the nanotubes is not obvious, which may be because they are well dispersed in the PE matrix. Fig. 3b compares nanocomposites with different contents of m-CNTs. It should be pointed out that the addition of the m-CNT nanofiller does not change the crystallization characteristics. With the increase in carbon nanotube filler content, the peak position of the polyethylene remains

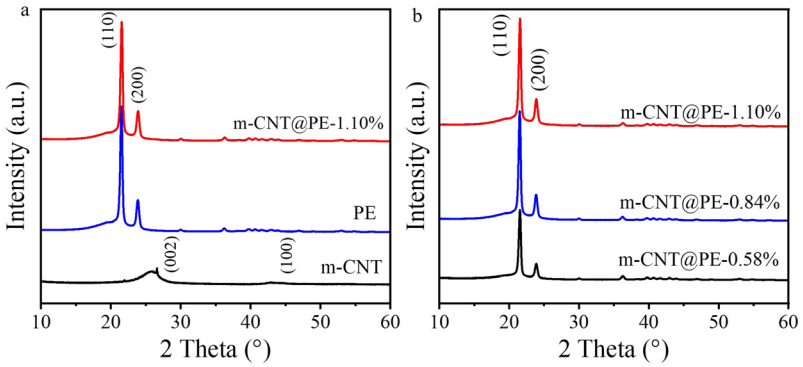

Fig. 3 (a) XRD patterns of the CNT/PE nanocomposite, PE and CNT. (b) XRD patterns of the nanocomposites with increasing CNT content.

unchanged, only with the half peak width of the (110) crystal plane becoming narrowed, which may support a slight enhancement in crystallization.

As shown in the XRD results, PE is a partially crystalline polymer. Fig. 4a shows the DSC melting curves of the nanocomposites. The melting peak temperature of the samples shows a little increase with increasing m-CNT content. Also, the enthalpy values of the nanocomposites have increased. The calculated melting enthalpies are 138.55 J g^{-1}, 140.29 J g^{-1}, 141.71 J g^{-1} and 149.25 J g^{-1}, respectively, for pure polyethylene, and 0.58 wt%, 0.84 wt% and 1.10 wt% CNT/PE nanocomposites. The results support the idea that the degree of crystallinity of PE can be enhanced by the introduction of CNTs.

Fig. 5a shows the stress–strain curves for pure PE and the nanocomposites. Compared with pure PE, the elongation at break of the composites shows no obvious decrease, while the yield stress of the composites with 0.58 wt%, 0.84 wt% and 1.10 wt% m-CNTs is increased to 18.40 MPa, 19.42 MPa and 20.76 MPa, respectively (Fig. 5b). The yield stress has increased by 1.94%, 7.59% and 15.02%, respectively. Fig. 5c further compares the Young's modulus of PE and the nanocomposites. The Young's modulus of the composite has increased from 128.42 MPa to 137.21 MPa, 142.15 MPa and 147.54 MPa, respectively (Fig. 5c), consistent with the enhanced mechanical strength. The increased mechanical properties support the finding that the m-CNTs have been uniformly dispersed into the PE matrix and bond well with it. The modified carbon nanotubes can play an effective role in stress transfer in the PE matrix.

The strengthening effect of the CNTs on PE not only increases the yield stress, but also enhances the toughness of PE. Fig. 5d shows a comparison of the impact toughness of the nanocomposites. According to the test results, the impact toughness of pure PE is 33.85 kJ m^{-2}, and that of the nanocomposites with 0.58 wt%, 0.84 wt% and 1.096 wt% CNTs is improved to 34.93 kJ m^{-2}, 36.28 kJ m^{-2} and 37.89 kJ m^{-2}, respectively, in which the impact toughness of the 1.10 wt% nanocomposite has increased by 11.94%. It can be seen that with an increase in carbon nanotube content in the PE matrix, the comprehensive mechanical properties show a rising trend on the whole. The impact toughness of the nanocomposites convincingly shows that the m-CNTs interact well with the PE matrix, and the stress is transferred to the carbon nanotube bundle through the matrix. The CNTs in the matrix play a bridging role to disperse the load stress, delay tear stress leading to destruction of the composites, and improve the impact toughness of the composites.

Fig. 6a shows that the cross-section of PE is a wave-shaped layered crystal. After adding different m-CNTs into the PE matrix, the PE crystals become much smaller, as shown in Fig. 6b–d. Meanwhile, with an increase in nanotube filler, the

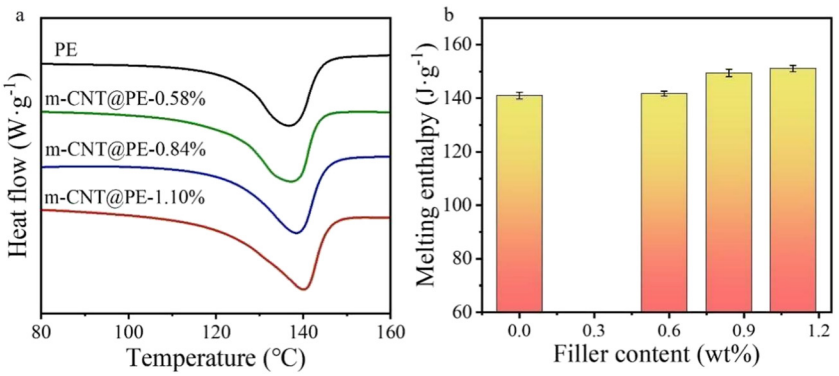

Fig. 4 Comparison of (a) DSC melting curves and (b) enthalpy values of the nanocomposites with increasing m-CNT content.

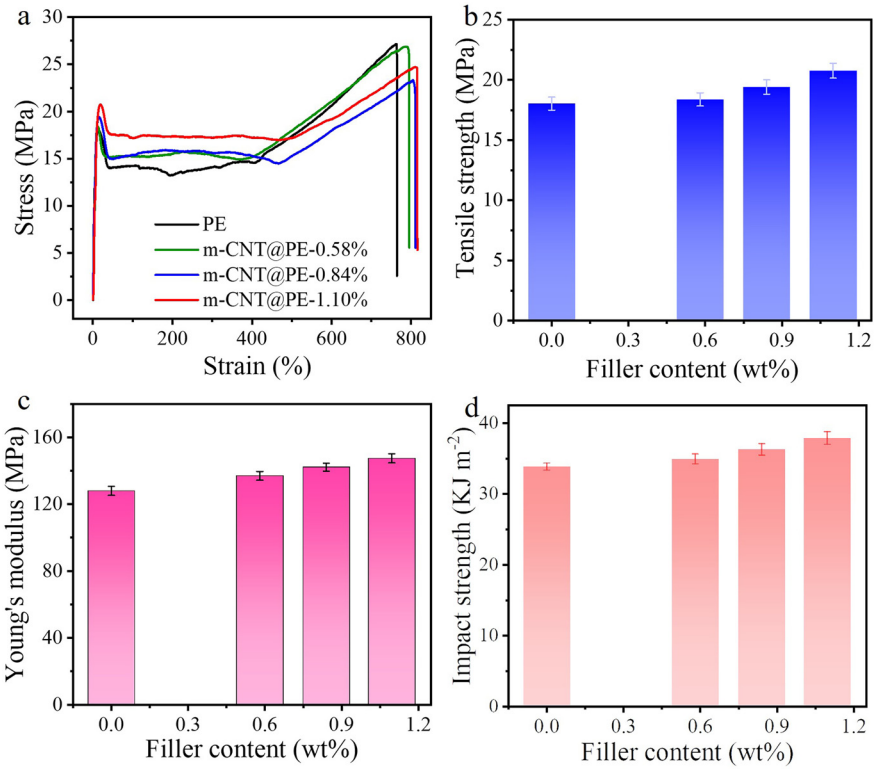

Fig. 5 (a) Stress–strain curves; (b) yield stress; (c) Young's modulus; and (d) impact toughness of PE and CNT/PE nanocomposites.

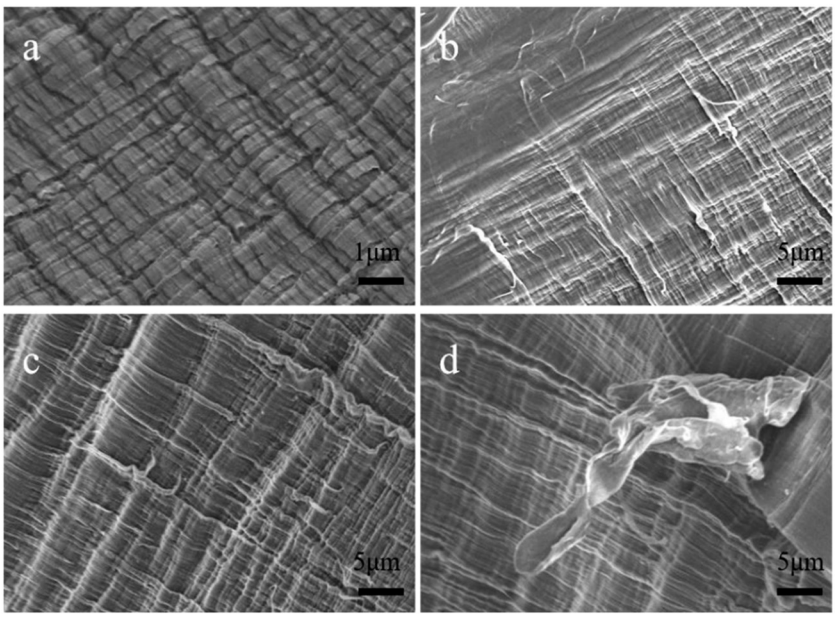

Fig. 6 Cross-sectional SEM images of the materials: (a) PE; (b) 0.58 wt%; (c) 0.84 wt%; (d) 1.10 wt% CNT/PE nanocomposites.

layered crystal structure of the PE matrix becomes smaller. This supports the idea that the added m-CNTs can act as grain refiners to toughen the PE, consistent with the increase in mechanical strength of the nanocomposites. Moreover, the fracture surface of the CNT/PE nanocomposites is rough, with no CNTs observed being pulled out of the PE matrix, and there is no obvious phenomenon of large particle agglomeration. The results indicate that the CNTs hinder the cracking of the PE matrix.

Fig. 7 and 8 compare the fouling formation on pure PE and the 1.10 wt% CNT/PE nanocomposite. During this observation period, polarized microscopy shows that the

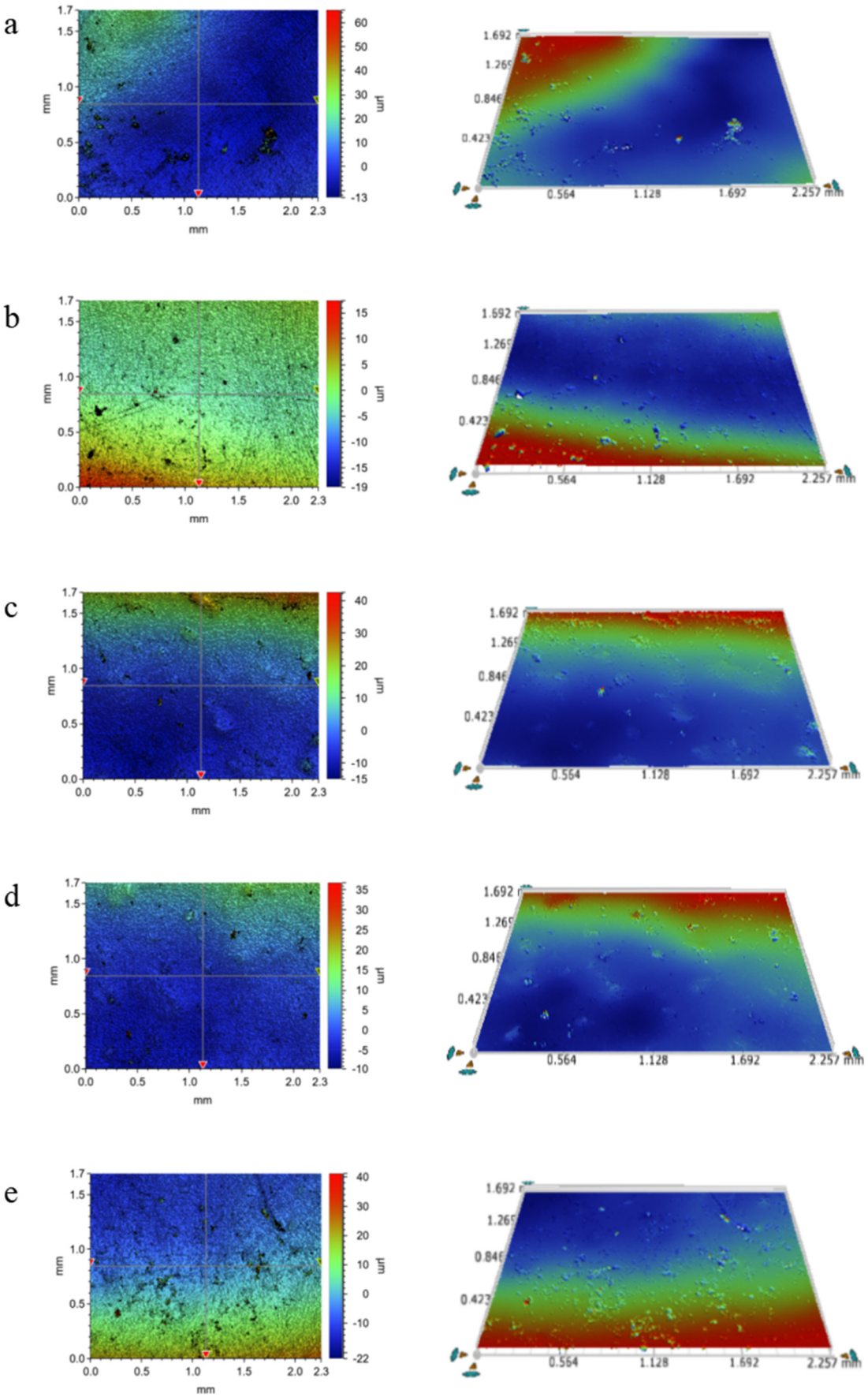

Fig. 7 (a–e) Surface morphology (left) of a pure PE sample soaked in oilfield water for 10, 17, 24, 31 and 38 days, respectively, and the 3D topography (right) after flattening.

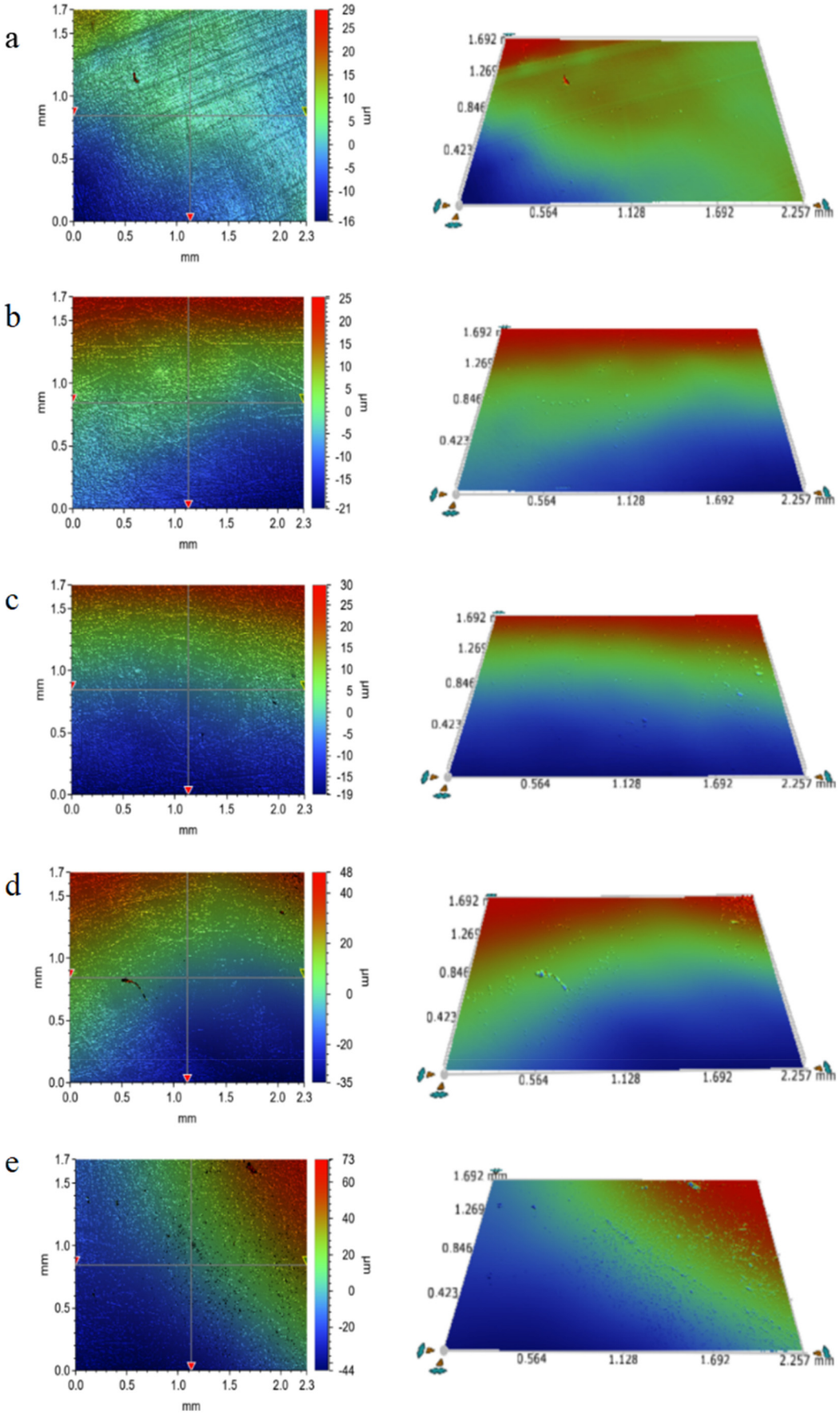

Fig. 8 (a–e) Surface morphology (left) and 3D morphology (right) of the 1.10 wt% CNT/PE nanocomposite after being soaked in oilfield water for 10, 17, 24, 31 and 38 days, respectively.

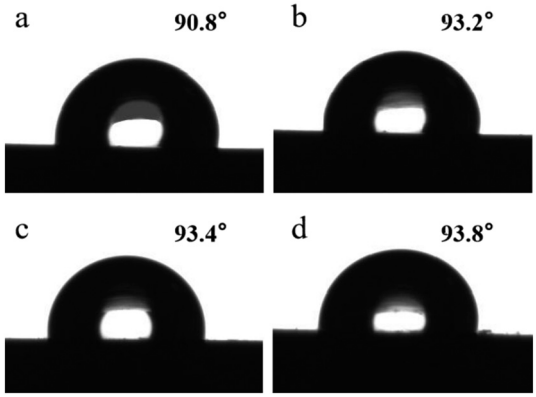

Fig. 9 Surface contact angle of PE and the nanocomposites: (a) PE sample; (b–d) 0.58 wt%, 0.84 wt%, and 1.10 wt% CNT/PE nanocomposites.

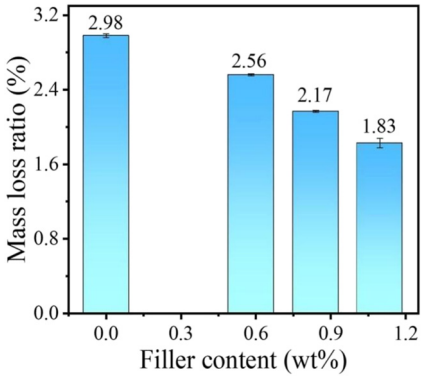

Fig. 10 Comparison of the mass loss of PE and the CNT/PE nanocomposite after corrosion.

CNT/PE nanocomposite displays less scale and fewer corrosion hole defects on the surface for the same time soaking in oilfield water. The results indicate that adding a certain amount of CNTs to PE can effectively inhibit the formation of scale and enhance the corrosion resistance of the PE matrix. The reason why the scaling on the surface of the composite material may be reduced should be related to the surface free energy of the nanocomposite material decreasing when the CNTs are added.

Fig. 9 shows that the surface contact angle of pure PE is 90.8°, indicating that PE is a hydrophobic material. After adding CNTs into the PE matrix, the surface contact angle of all the nanocomposite materials has increased a little. The surface contact angles become 93.2°, 93.4°, and 93.8° for the 0.58 wt%, 0.84 wt%, and 1.10 wt% CNT/PE nanocomposites, respectively. The results support the idea that the hydrophobic property of PE has been enhanced with the increase in CNTs. The surface energy of polyethylene is 35.5 mJ m^{-2}. It can be calculated that the surface energy of the composite material with 1.10 wt% CNTs is 29.65 mJ m^{-2}, which is 16.47% lower than that of pure PE. Therefore, it becomes more difficult for impurities in water to be adsorbed on the surface of the material, avoiding the accumulation of dirt, which can bring about better anti-scaling performance.

To further confirm the anti-corrosion property, PE and CNT/PE nanocomposites of the same size were soaked in a concentrated sulfuric acid–hydrochloric acid (1 : 1 in volume) corrosive solution (80 °C, 5 min). After that, the mass loss of the samples was calculated and is shown in Fig. 10. Compared with pure PE, the mass loss of all the nanocomposite materials is less after corrosion in an acidic environment, which indicates that the addition of CNTs plays a reinforcing role in the PE matrix, consistent with the results for increased crystallinity.

3 Conclusions

In summary, PE nanocomposites have been prepared by the introduction of m-CNTs into the PE matrix, which provide improved anti-scaling and corrosion-resistant properties, as well as increased mechanical properties. For better interface compatibility, the CNTs were treated with nitric acid oxidation and reactive tetrabutyl titanate, to obtain a uniform dispersion and intimate interface interaction. With an increase in the m-CNT fraction, the crystallinity of PE displays an increase and the surface free energy of the composite materials decreases. As a result, the scaling on the surface of the composite material is obviously reduced compared with pure PE, and the nanocomposites become more corrosion resistant. Moreover, due to the good dispersion, the composites show enhanced mechanical properties. That is, by adding 1.10 wt% m-CNTs, the tensile stress and impact toughness of the composites are 20.76 MPa and 37.89 kJ m^{-2}, respectively, increases of 15.0% and 11.9% compared with pure PE. This paper supports the idea that the crystallinity of the PE matrix can be improved by adding CNTs, thereby increasing its corrosion resistance and anti-scaling properties. It has broad prospects in oilfield production and other industrial applications.

4 Experimental section

4.1 Materials

The CNTs were prepared by chemical vapor deposition using a fluidized bed reactor. They were multi-walled CNTs with lengths of more than 10 microns and diameters of 7–11 nanometers. Polyethylene was provided by Petrochina Daqing Chemical Research Center. Ethanol, nitric acid and tetrabutyl titanate were analytically pure and were purchased from Sinopharm Group Chemical Reagents Co., Ltd.

4.2 Modification of the CNTs

First, 200 g of the as-prepared CNT powder was mixed into 7% nitric acid solution. Then the mixture was stirred for 1 hour with a magnetic stirrer. After that, the nitric acid treated CNTs were collected from the suction filter by washing with ultrapure water until the filtrate became neutral. After drying in an oven for 24 hours, we had CNTs oxidized by nitric acid. Subsequently, 5 wt% tetrabutyl titanate–ethanol solution was

prepared, and 100 g of the HNO_3-oxided CNT was weighed and mixed into 2.5 L of the prepared tetrabutyl titanate–ethanol solution. Then the mixture was continuously stirred for 1.5 hours with a magnetic stirrer. After that, the CNTs were washed with ethanol and filtered with a suction filter funnel. After drying for 12 hours in an oven, the tetrabutyl titanate modified CNTs were obtained.

4.3 Melt extrusion-hot pressing of the nanocomposites

PE and the modified CNTs were mixed with an SJZ-45 experimental twin screw extruder at 210 °C. They were extruded according to the three weight proportions of 200 : 1.16, 200 : 1.69 and 200 : 2.21. The corresponding nanocomposites were PE/CNT pellets of 0.58 wt%, 0.84 wt% and 1.10 wt%, respectively.

4.4 Characterization

SEM experiments were conducted on a JEOL-2010 at 3.0 kV. TEM experiments were conducted on the JEM-2010 operated at 120 kV. Raman spectra were performed on a HR800 inVia with He–Ne laser excitation at 532 nm. The tensile properties of the samples were analyzed with a universal tensile testing machine MTS (SANS) CMT4502. The samples were dog-bone shaped with tested length, width and thickness of 20 mm, 4 mm and 2 mm, respectively. The tensile speed was 10 mm min^{-1}. The impact toughness of the samples was analyzed with a JB-25 pendulum impact tester, and the samples were Charpy V-notch impact samples. Thermal analysis (TGA test, Q5000 IR) was used to obtain the thermal properties of the composites at a heating rate of 10 °C min^{-1} under nitrogen. The crystallization properties of the composites were obtained at room temperature with a heating rate of 10 °C min^{-1} with a DSC6200 from SEIKO Instrument Company, Japan. An XPS-Kratos-AXIS X-ray photoelectron spectrometer manufactured by the Spike Company of Germany was used to further study the surface structure of the CNTs. A white light interference three-dimensional microscope (Contour GTK) was used to analyze the dirt morphology and corrosion pits on the sample surface. The wetting angle of the composite surface was measured with an SL200B contact angle meter.

Conflicts of interest

The authors declare no competing financial interest.

Acknowledgements

This work was supported by the research fund of China National Petroleum Corporation (No. 2020E-2801(GF)).

References

1 A. Benamor, A. G. Talkhan, M. Nasser, I. Hussein and P. C. Okonkwo, Effect of temperature and fluid speed on the corrosion behavior of carbon steel pipeline in Qatari oilfield produced water, *J. Electroanal. Chem.*, 2018, **808**, 218–227.
2 A. A. Olajire, A review of oilfield scale management technology for oil and gas production, *J. Pet. Sci. Eng.*, 2015, **135**, 723–737.
3 M. El-Said, M. Ramzi and T. Abdel-Moghny, Analysis of oilfield waters by ion chromatography to determine the composition of scale deposition, *Desalination*, 2009, **249**, 748–756.
4 A. B. BinMerdhah, A. A. M. Yassin and M. A. Muherei, Laboratory and prediction of barium sulfate scaling at high-barium formation water, *J. Pet. Sci. Eng.*, 2010, **70**, 79–88.
5 Y. Dong, Analysis on anti-corrosion and anti-scaling technology of water injection well in oil production plant, *IOP Conf. Ser. Earth Environ. Sci.*, 2020, **514**, 022005.
6 B. Dong, Y. Xu, H. Deng, F. Luo and S. Jiang, Effects of pipeline corrosion on the injection water quality of low permeability in oilfield, *Desalination*, 2013, **326**, 141–147.
7 G. Pei, C. Wang and L. Liu, Experimental study on the cause of inorganic scale formation in the water injection pipeline of tarim oilfield, *J. Chem.*, 2014, **2014**, 619834.
8 S. Pourhashem, A. Seif, F. Saba, E. G. Nezhad, X. Ji, Z. Zhou, X. Zhai, M. Mirzaee, J. Duan, A. Rashidi and B. Hou, Antifouling nanocomposite polymer coatings for marine applications: A review on experiments, mechanisms, and theoretical studies, *J. Mater. Sci. Technol.*, 2022, **118**, 73–113.
9 M. F. Montemor, Functional and smart coatings for corrosion protection: A review of recent advances, *Surf. Coat. Technol.*, 2014, **258**, 17–37.
10 L. Rassouli, R. Naderi and M. Mahdavain, The role of micro/nano zeolites doped with zinc cations in the active protection of epoxy ester coating, *Appl. Surf. Sci.*, 2017, **423**, 571–583.
11 R. Fürstner, W. Barthlott, C. Neinhuis and P. Walzel, Wetting and self-cleaning properties of artificial superhydrophobic surfaces, *Langmuir*, 2005, **21**, 956–961.
12 T. Zhu, X. Li, X. Zhao, X. Zhang, Y. Lu and L. Zhang, Stress-strain behavior and corresponding crystalline structures of four types of polyethylene under a wide range of strain rates, *Polym. Test.*, 2022, **106**, 107460.
13 S. V. Harb, S. H. Pulcinelli, C. V. Santilli, K. M. Knowles and P. A. Hammer, Comparative study on graphene oxide and carbon nanotube reinforcement of PMMA-siloxane-silica anticorrosive coatings, *ACS Appl. Mater. Interfaces*, 2016, **8**, 16339–16350.
14 I. Hejazi, B. Hajalizadeh, J. Seyfi, G. M. M. Sadeghi, S.-H. Jafari and H. A. Khonakdar, Role of nanoparticles in phase separation and final morphology of superhydrophobic polypropylene/zinc oxide nanocomposite surfaces, *Appl. Surf. Sci.*, 2014, **293**, 116–123.
15 J. Seyfi, I. Hejazi, S.-H. Jafari, H. A. Khonakdar, G. M. Mohamad Sadeghi, A. Calvimontes and F. Simon, On the combined use of nanoparticles and a proper solvent/non-solvent system in preparation of superhydrophobic polymer coatings, *Polymer*, 2015, **56**, 358–367.
16 N. Lachman and H. Daniel Wagner, Correlation between interfacial molecular structure and mechanics in CNT/epoxy nano-composites, *Composites, Part A*, 2010, **41**, 1093–1098.

17 R. Pratyush Behera, P. Rawat, S. Kumar Tiwari and K. Kumar Singh, A brief review on the mechanical properties of Carbon nanotube reinforced polymer composites, *Mater. Today: Proc.*, 2020, **22**, 2109–2117.
18 Y. Lu, L. Liu, M. Tian, H. Geng and L. Zhang, Study on mechanical properties of elastomers reinforced by zinc dimethacrylate, *Eur. Polym. J.*, 2005, **41**, 589–598.
19 Q. Zhang, J.-Q. Huang, W.-Z. Qian, Y.-Y. Zhang and F. Wei, The road for nanomaterials industry: A review of carbon nanotube production, post-treatment, and bulk applications for composites and energy storage, *Small*, 2013, **9**, 1237–1265.
20 M. Khoshsefat, A. Dechal, S. Ahmadjo, S. M. M. Mortazavi, G. Zohuri and J. B. P. Soares, Amorphous to high crystalline PE made by mono and dinuclear Fe-based catalysts, *Eur. Polym. J.*, 2019, **119**, 229–238.
21 W. Tang, M. H. Santare and S. G. Advani, Melt processing and mechanical property characterization of multi-walled carbon nanotube/high density polyethylene(MWNT/HDPE) composite films, *Carbon*, 2003, **41**, 2779–2785.
22 D. Bikiaris, A. Vassiliou, K. Chrissafis, K. M. Paraskevopoulos, A. Jannakoudakis and A. Docoslis, Effect of acid treated multi-walled carbon nanotubes on the mechanical, permeability, thermal properties and thermo-oxidative stability of isotactic polypropylene, *Polym. Degrad. Stab.*, 2008, **93**, 952–967.
23 H. Meng, G. X. Sui, P. F. Fang and R. Yang, Effects of acid- and diamine-modified MWNTs on the mechanical properties and crystallization behavior of polyamide 6, *Polymer*, 2008, **49**, 610–620.
24 D. Zhao, Q. Lei, C. Qin and X. Bai, Melt process and performance of multi-walled carbon nanotubes reinforced LDPE composites, *Pigm. Resin Technol.*, 2006, **35**(6), 341–345.
25 M. M. Zamani, A. Fereidoon and A. Sabet, Multi-walled carbon nanotube-filled polypropylene nanocomposites: High velocity impact response and mechanical properties, *Iran. Polym. J.*, 2012, **21**, 887–894.
26 M. Cadek, J. N. Coleman, K. P. Ryan, V. Nicolosi, G. Bister, A. Fonseca, J. B. Nagy, F. Béguin, K. Szostak and W. J. Blau, Reinforcement of polymers with carbon nanotubes: The role of nanotube surface area, *Nano Lett.*, 2004, **4**(2), 353–356.
27 X. Jia, Q. Zhang, M.-Q. Zhao, G.-H. Xu, J.-Q. Huang, W. Qian, Y. Lu and F. Wei, Dramatic enhancements in toughness of polyimide nanocomposite via long-CNT-induced long-range creep, *J. Mater. Chem.*, 2012, **22**(14), 7050–7056.
28 B. M. Amoli, S. A. A. Ramazani and H. Izadi, Preparation of ultrahigh-molecular-weight polyethylene/carbon nanotube nanocomposites with a Ziegler–Natta catalytic system and investigation of their thermal and mechanical properties, *J. Appl. Polym. Sci.*, 2012, **125**, E453–E461.
29 J. Yap, M. J. Fuller, L. A. Schafer and S. Kelkar, Removing iron sulfide scale: A novel approach, in *Abu Dhabi International Petroleum Exhibition and Conference*, 2010, p. SPE-138520-MS.
30 D. S. Lakshmi, B. Senthilmurugan, E. Drioli and A. Figoli, Application of ionic liquid polymeric microsphere in oil field scale control process, *J. Pet. Sci. Eng.*, 2013, **112**, 69–77.
31 B. Senthilmurugan, B. Ghosh and S. Sanker, High performance maleic acid based oil well scale inhibitors-development and comparative evaluation, *J. Ind. Eng. Chem.*, 2011, **17**, 415–420.
32 N. Salah, A. M. Alfawzan, A. Saeed, A. Alshahrie and W. Allafi, Effective reinforcements for thermoplastics based on carbon nanotubes of oil fly ash, *Sci. Rep.*, 2019, **9**, 20288.
33 H. Fouad, R. Elleithy, S. M. Al-Zahrani and M. A.-H. Ali, Characterization and processing of high density polyethylene/carbon nano-composites, *Mater. Des.*, 2011, **32**, 1974–1980.
34 R. T. Tebeta, A. M. Fattahi and N. A. Ahmed, Experimental and numerical study on HDPE/SWCNT nanocomposite elastic properties considering the processing techniques effect, *Microsyst. Technol.*, 2020, **26**, 2423–2441.
35 H. Hiura, T. W. Ebbesen and K. Tanigaki, Opening and purification of carbon nanotubes in high yields, *Adv. Mater.*, 1995, **7**(3), 275–276.
36 H. Shen, J. Guo, H. Wang, N. Zhao and J. Xu, Bioinspired modification of h-BN for high thermal conductive composite films with aligned structure, *ACS Appl. Mater. Interfaces*, 2015, **7**, 5701–5708.
37 T. Ramanathan, A. A. Abdala, S. Stankovich, D. A. Dikin, M. Herrera-Alonso, R. D. Piner, D. H. Adamson, H. C. Schniepp, X. Chen, R. S. Ruoff, S. T. Nguyen, I. A. Aksay, R. K. Prud'Homme and L. C. Brinson, Functionalized graphene sheets for polymer nanocomposites, *Nat. Nanotechnol.*, 2008, **3**, 327–331.
38 B. Ge, Z. Zhang, X. Zhu, X. Men, X. Zhou and Q. Xue, A graphene coated cotton for oil/water separation, *Compos. Sci. Technol.*, 2014, **102**, 100–105.
39 K. Esumi, M. Ishigami, A. Nakajima, K. Sawada and H. Honda, Chemical treatment of carbon nanotubes, *Carbon*, 1996, **34**, 279–281.
40 X. Wang, Z. Z. Yong, Q. W. Li, P. D. Bradford, W. Liu, D. S. Tucker, W. Cai, H. Wang, F. G. Yuan and Y. T. Zhu, Ultrastrong, stiff and multifunctional carbon nanotube composites, *Mater. Res. Lett.*, 2013, **1**, 19–25.
41 K. Jiang, Q. Li and S. Fan, Spinning continuous carbon nanotube yarns, *Nature*, 2002, **419**, 801–801.
42 T. Yamamoto and K. Kawaguchi, Synthesis of composite polymer particles with carbon nanotubes and evaluation of their mechanical properties, *Colloids Surf., A*, 2017, **529**, 765–770.
43 A. V. Desai and M. A. Haque, Mechanics of the interface for carbon nanotube–polymer composites, *Thin Walled Struct.*, 2005, **43**, 1787–1803.
44 B. A. I. Jinbo, Evidence of the reinforcement role of chemical vapour deposition multi-walled carbon nanotubes in a polymer matrix, *Carbon*, 2003, **41**, 1325–1328.
45 W.-H. Li, X.-H. Chen, Z. Yang and L.-S. Xu, Structure and properties of polypropylene-wrapped carbon nanotubes composite, *J. Appl. Polym. Sci.*, 2009, **113**, 3809–3814.
46 A. A. Zdanovich, S. I. Moseenkov, A. V. Ishchenko, V. L. Kuznetsov, M. A. Matsko and V. A. Zakharov, The morphology evolution of polyethylene produced in the presence of a Ziegler-type catalyst anchored on the surface

of multi-walled carbon nanotubes, *J. Appl. Polym. Sci.*, 2021, **138**, 50528.

47 M. Nisar, C. P. Bergmann, J. Geshev, R. Quijada, T. Maraschin, N. R. de Souza Basso, E. G. Barrera and G. B. Galland, Synthesis of high-density polyethylene/rGO-CNT-Fe nanocomposites with outstanding magnetic and electrical properties, *J. Appl. Polym. Sci.*, 2017, **134**, 45382.

48 L. Li, H. Shi, Z. Liu, L. Mi, G. Zheng, C. Liu, K. Dai and C. Shen, Anisotropic conductive polymer composites based on high density polyethylene/carbon nanotube/polyoxyethylene mixtures for microcircuits interconnection and organic vapor sensor, *ACS Appl. Nano Mater.*, 2019, **2**, 3636–3647.

49 E. Erfanian, M. Kamkar, D. Williams, Y. Zamani Keteklahijani, R. Salehiyan, S. S. Ray, M. Arjmand and U. Sundararaj, Dielectrorheology of aspect-ratio-tailored carbon nanotube/polyethylene composites under large deformations: Implications for high-temperature dielectrics, *ACS Appl. Nano Mater.*, 2021, **4**, 11493–11504.

50 Z. Wu, H. Wang, M. Xue, X. Tian, X. Ye, H. Zhou and Z. Cui, Facile preparation of superhydrophobic surfaces with enhanced releasing negative air ions by a simple spraying method, *Compos. Sci. Technol.*, 2014, **94**, 111–116.

51 J. Yang, Z. Zhang, X. Men and X. Xu, Fabrication of stable, transparent and superhydrophobic nanocomposite films with polystyrene functionalized carbon nanotubes, *Appl. Surf. Sci.*, 2009, **255**, 9244–9247.

52 C.-F. Wang, W.-Y. Chen, H.-Z. Cheng and S.-L. Fu, Pressure-proof superhydrophobic films from flexible carbon nanotube/polymer coatings, *J. Phys. Chem. C*, 2010, **114**, 15607–15611.

53 S. Sethi, L. Ge, L. Ci, P. M. Ajayan and A. Dhinojwala, Gecko-inspired carbon nanotube-based self-cleaning adhesives, *Nano Lett.*, 2008, **8**, 822–825.

54 I. Hejazi, G. M. M. Sadeghi, S. H. Jafari, H. A. Khonakdar, J. Seyfi, M. Holzschuh and F. Simon, Transforming an intrinsically hydrophilic polymer to a robust self-cleaning superhydrophobic coating via carbon nanotube surface embedding, *Mater. Des.*, 2015, **86**, 338–346.

55 S. Sethi and A. Dhinojwala, Superhydrophobic conductive carbon nanotube coatings for steel, *Langmuir*, 2009, **25**, 4311–4313.

56 S. Imtiaz, M. Siddiq, A. Kausar, S. T. Muntha, J. Ambreen and I. Bibi, A Review Featuring Fabrication, Properties and Applications of Carbon Nanotubes(CNTs) Reinforced Polymer and Epoxy Nanocomposites, *Chin. J. Polym. Sci.*, 2018, **36**, 445–461.

57 C. M. Vu and Q. V. Bach, Oxidized multiwall carbon nanotubes filled epoxy-based coating: fabrication, anticorrosive, and mechanical characteristics, *Polym. Bull.*, 2021, **78**, 2329–2339.

58 M. Omastová, J. Prokeš, S. Podhradská and I. Chodák, Stability of electrical and mechanical properties of polyethylene/carbon black composites, *Macromol. Symp.*, 2001, **170**, 231–240.

59 J. L. Sullivan, S. O. Saied and I. Bertoti, Effect of ion and neutral sputtering on single crystal TiO_2, *Vacuum*, 1991, **42**, 1203–1208.